論文 / 著書情報
Article / Book Information

Title	Observation of turnover of spontaneous polarization in ferroelectric layer of pentacene/poly-(vinylidene-trifluoroethylene) double-layer capacitor under photo illumination by optical second-harmonic generation measurement
Authors	Zhemin Shi, Dai Taguchi, Takaaki Manaka, Mitsumasa Iwamoto
Citation	Journal of Applied Physics, 119, , 165502/1-7
Pub. date	2016, 4
Note	This article may be downloaded for personal use only. Any other use requires prior permission of the author and AIP Publishing. The following article appeared in Journal of Applied Physics, 119, , 165502/1-7 and may be found at http://dx.doi.org/10.1063/1.4947584.
Note	This file is author (final) version.

Direct probing of photo illumination effect on turnover of spontaneous polarization in ferroelectric layer of pentacene/poly-(vinylidene-trifluoroethylene) double-layer capacitor by electric-field-induced optical second-harmonic generation measurement

Zhemin Shi[a,b], Dai Taguchi[b], Takaaki Manaka[b], and Mitsumasa Iwamoto[b]

[a]*State Key Laboratory of New Ceramics and Fine Processing, School of Materials Science and Technology, Tsinghua University, Beijing 100084，China*

[b]*Department of Physical Electronics, Tokyo Institute of Technology, 2-12-1 O-okayama, Meguro-ku, Tokyo 152-8552, Japan*

Phone: +81-3-5734-2191

E-mail: iwamoto@pe.titech.ac.jp

Abstract

The details of turnover process of spontaneous polarization and associated carrier motions in Indium-tin oxide (ITO)/Poly-(vinylidene-trifluoroethylene) [P(VDF-TrFE)]/Pentacene/Au capacitor were analyzed by coupling displacement current measurement (DCM) and electric-field-induced optical second-harmonic generation (EFISHG) measurement. A model was set up from DCM results to depict the relationship between electric filed in semiconductor layer and applied external voltage, proving that photo illumination effect on spontaneous polarization process lied in variation of semiconductor conductivity. The EFISHG measurement directly and selectively probed the electric field distribution in semiconductor layer, modifying the model and revealing detailed carrier behaviors involving photo illumination effect, dipole reversal, and interfacial charging in the device. Further decrease of DCM current in the low voltage region under illumination was found as the result of illumination effect, and the result was argued based on the changing of the total capacitance of the double-layer capacitors.

Key words: EFISHG; dipole reversal; model; carrier behavior; photo illumination

Ⅰ. INTRODUCTION

Much attention has been paid to turn-over of spontaneous polarization of ferroelectric materials for application to memory devices [1-3], but currently, researchers are also paying their attention to the usage of internal electric field induced by spontaneous polarization in ferroelectric materials [4,5], for improvement of efficiency of Organic Solar Cell (OSCs) and other devices. Among them, ferroelectric organic films, especially poly-(vinylidene fluoride-trifluoroethylene) [P(VDF-TrFE)], shows advantageous qualities, such as high density, aligned dipole orientation, solution processability, low fabrication temperature, high chemical stability as well as compatibility with semiconducting materials [6-9]. Besides, researchers have confirmed the efficiency enhancement of OSCs devices by employing the local electric field generated from dipole reversal in inserted symmetric ultra-thin P(VDF-TrFE) film [4]. However, the distribution of electric filed induced by unscreened polarization charges inside the device is still not clear. Electric-field-induced optical second-harmonic generation (EFISHG) measurement can selectively and directly probe the electric field in organic semiconductor layer, which makes it available to visualize space charge distribution in organic devices using ferroelectric layer [10-12]. This motivates us to study the turn-over process of

spontaneous polarization and associated carrier motions in Indium-tin oxide (ITO)/ P(VDF-TrFE)/Pentacene/Au double-layer capacitors.

In our previous studies on this pentacene/P(VDF-TrFE) double layer capacitors in dark [13-15], a two-step polarization process was proposed and a Maxwell-Wargner (MW) model was set up to visualize electric field-voltage plot converted from I-V characteristics. However, the model was only partly adoptable, since though the hysteresis loops positions incorporated according to C-V results made sense, the detailed loops directions failed to match the reported EFISHG results completely [15]. In addition, for enough high light intensity, internal fields by photogenerated carrier impacted the polarization reversal process [16]. But to what extent did the space charge field compensate the potential drop across the pentacene layer was still ambiguous. Therefore, modifying the model for exploring detailed carrier motions to reveal space charge distribution collaborated by dipole reversal, interfacial charging/discharging, and photo illumination effect is necessary.

In this study, a Metal-Ferroelectric-Semiconductor-Metal (MFSM) device with/without illumination effect was carefully studied. A model was forwarded based on dielectric physics deriving from displacement current measurement (DCM). It detects the origins of internal electric field in semiconductor layer and describes the variation of the local electric field with external applied voltage, revealing more details of carrier motions with photo illumination effect by coupling EFISHG measurement.

Ⅱ. EXPERIMENT

Sample Preparation

Fig.1 shows the MFSM double layer capacitor used in the experiment, with P(VDF-TrFE) as ferroelectric and pentacene as semiconductor. P(VDF-TrFE) (70/30, mol%) film with a thickness of 350 nm was spin-coated on a pre-cleaned ITO substrate, in the manner same as in Ref. 13, followed by annealing at 135℃ for 2h in dry nitrogen atmosphere for high crystallinity and stabilized texture [17, 18]. Afterwards, pentacene layer (150 nm) and gold electrode (100 nm) were sequentially thermal evaporated at a vacuum below 10^{-3} Pa, with the deposition rate of pentacene layer controlled at 0.7 Å/s using a quartz crystal microbalance (QCM). The device working area was approximately 3.1 mm^2. Here to mention that single layer device, Metal-Ferroelectric-Metal (MFM) device, was also prepared for comparison. Noteworthy that, there is no mixing between pentacene layer and P(VDF-TrFE) layer during thermal evaporation at controlled speed.

DCM and EFISHG

For the DCM measurement, a ramp voltage was applied on the ITO electrode with reference to the gold electrode in a manner as $0 \rightarrow -V_m \rightarrow V_m \rightarrow 0$ (V_m was the amplitude and equaled to 60 V, see Fig. 1), which is generated from a function generator (NF WF1974) and then amplified with a power amplifier (NF HSA4101). The current-voltage (I-V) characteristics were recorded using two electrometers (Keithley 6517 and Digital multimeter 2000). A white light from a light-emitting diode with an intensity of 6 mW/cm^2 was used as a light source to generate photocarriers in pentacene layer through fully transparent P(VDF-TrFE) layer from the ITO side [19], as depicted in Fig.1.

According to the Maxwell-Wagner effect, the charge accumulation at the interface is governed by the relaxation time τ ($\tau = \varepsilon / \sigma$, where ε is the dielectric constant and σ is the conductivity of the organic material) difference between two adjacent organic layers. Consequently, under the short-circuit condition, excess charges Q_s accumulated at the P(VDF-TrFE)/Pentacene interface. The total charge density in the area on the

upper and lower electrode surfaces (Q_1 and Q_2, as shown in Fig. 1) can be respectively written as

$$Q_1 = -CV - \frac{P+Q_s}{C_1+C_2}C_1 \tag{1a}$$

and

$$Q_2 = CV - \frac{P+Q_s}{C_1+C_2}C_2 + P\,. \tag{1b}$$

Here C_1 and C_2 are the capacitance density of pentacene layer (layer 1) and P(VDF-TrFE) layer (layer 2), respectively, and $C=C_1C_2/(C_1+C_2)$ is the total capacitance density in series, P is the remenant polarization of layer 2. Noteworthy that P is defined positive when dipoles in P(VDF-TrFE) layer is oriented upwards in a manner as illustrated in Fig. 1, Q_s is set as positive when holes are accumulated at the interface. Due to the inherent dielectric property of both P(VDF-TrFE) and pentacene layers, merely small amount of intrinsic free carriers are allowed to be transported through the layers, but it is negligibly small. Therefore, by substituting Eq. (1a), the detected current density flowing through the device can be written as,

$$I = -\frac{\partial Q_1}{\partial t} = C\frac{\partial V}{\partial t} + \frac{C_1}{C_1+C_2}\frac{\partial P}{\partial t} + \frac{C_1}{C_1+C_2}\frac{\partial Q_s}{\partial t}\,, \tag{2}$$

by assuming conduction current is discarded. Here, the first term $C\partial V/\partial t$ is constant and equals to $-4fCV_0$ or $4fCV_0$ (f and V_0 are the frequency and amplitude of the applied ramp voltage, respectively). The other two terms suggest that variation of Q_s and P are the contributing element to displacement current.

By applying the Gauss law of the Maxwell equation at the two interfaces between the electrode and dielectric layer, the boundary condition for both interfaces is written as,

$$0 - \varepsilon_1 E_1 = Q_1 \tag{3a}$$

and

$$\varepsilon_2 E_2 - 0 = Q_2 - P\,. \tag{3b}$$

Here ε_1 and ε_2, and E_1 and E_2 are the dielectric constants and average electrostatic local fields for layer 1 and layer 2, respectively. Noteworthy that the upward direction of the electric fields pictured in Fig. 1 is set as positive.

Replacing Q_1 in Eq. (1a) and Q_2 in Eq. (1b) with Eq. (3a) and Eq. (3b) respectively, we obtain the electric field across the layers

$$E_1 = \frac{CV}{\varepsilon_1} + \frac{P+Q_s}{C_1+C_2}\cdot\frac{1}{d} \tag{4a}$$

and

$$E_2 = \frac{CV}{\varepsilon_2} - \frac{P+Q_s}{C_1+C_2}\cdot\frac{1}{d_2}\,. \tag{4b}$$

E_1 is comprised of three parts, E_p, E_s and E_{ex}.

$$E_{ex} = \frac{C_1C_2}{C_1+C_2}\cdot\frac{V}{\varepsilon_1} \tag{5a}$$

$$E_s = \frac{Q_s}{C_1 + C_2} \cdot \frac{1}{d_1} \tag{5b}$$

$$E_p = \frac{P}{C_1 + C_2} \cdot \frac{1}{d_1} . \tag{5c}$$

Here, E_{ex} is the electric field originating from external applied voltage, E_s is the electric field originating from interfacial charge Q_s accumulated at pentacene/P(VDF-TrFE) interface, and E_p originates from the dipole moment P in the ferroelectric layer. Noteworthy that, we simplified the internal electric field in pentacene layer to be uniform distributed without considering the variation of carrier density or the impact of dipole moments along thickness of pentacene layer.

EFISHG measurement can directly probe the electric field E_1 by virtue of an optical arrangement as portrayed in Fig. 1. A wavelength of 860 nm was chosen to selectively probe the EFISHG signal from the pentacene layer at a wavelength of 430 nm, with negligible SHG signal from P(VDF-TrFE) layer [12,13,20]. By applying the same ramp voltage at the same frequency (10 mHz) as DCM measurement with laser irradiation, the second-harmonic (SH) intensity detected from the pentacene layer is given by [21]

$$I(2\omega) \propto d_1^2 \left|P(2\omega)\right|^2 = d_1^2 \left|\varepsilon_0 \chi^{(2)} : E(\omega) E(\omega) + \varepsilon_0 \chi^{(3)} : E_1 E(\omega) E(\omega)\right|^2 \tag{6}$$

where P(2ω) is the nonlinear polarization induced in pentacene layer, ε_0 is the vacuum permittivity, and $\chi^{(n)}$ (n=2,3) is the nth-order nonlinear susceptibility tensor, depending on the material of semiconductor. E_1 is the electrostatic local field in pentacene layer, and E(ω) is the electric field of incident laser beam. Noteworthy that, different from the Debye-Hückel approach [22], which is a microscopic technique to evaluate space distributions of charges in polymer films, we simply gathered the average SH signal of the spot size (< 1mm^2 [11]) in the pentacene layer via selectivity of EFISHG.

Due to the symmetric structure of applied pentacene layer, $\chi^{(2)}$ is assumed to be zero. Therefore, the laser induced SHG signal from pentacene is very insignificant without the enhancement from the external electric field, and thus $I(2\omega) \propto \left|E_1\right|^2$. Consequently, the EFISHG measurement probes variation of charges Q_s at the interface and dipole polarization P.

$$\sqrt{\Delta I(2\omega)} \propto \Delta E_1 = \frac{C}{\varepsilon_1} \cdot \Delta V + \frac{\Delta P}{C_1 + C_2} \cdot \frac{1}{d_1} + \frac{\Delta Q_s}{C_1 + C_2} \cdot \frac{1}{d_2} . \tag{7}$$

Ⅲ. RESULTS AND DISCUSSION

DCM results

Fig. 2 (a) shows the DCM results for MFM device and MFSM device. For MFM device, from reading the two symmetric peaks (peak R_1 at -15.34V and peak R_2 at 15.39V), we can derive the coercive electric field of the P(VDF-TrFE) ferro-layer as: $E_c = V_p / d_2 \approx 0.44$ MV/cm. These values agree well with previous reports [13, 23, 24].

For MFSM device in dark, a two-step polarization process appear with three peaks (peak 1 at -14.9V, peak 2 at 15.74V, and peak 3 at 30.32V), which indicates the conductivity change of pentacene layer [13, 14]. For MFSM device under illumination, there are only two symmetric peaks overlapped with peak 1 and peak 2 (peak1' at -14.9V, and peak 2' at 30.32V), suggesting that all the dipoles switch at once when electric field in P(VDF-TrFE) layer reaches to the coercive electric field.

From the perspective of dielectric physics, if semiconductor layer is conductive like metal, the turn-over voltage of dipoles, or rather, the peak position in DCM, $V_{T1}= E_c \cdot d_2=15.4$ V; If semiconductor layer is serving like insulator, $V_{T2}= E_c \cdot d_2 \cdot (C_1+C_2)/C_1 \approx 31.9$V. The speculated V_{T1} quite matches the position of peak 1, peak 2, peak 1'， and peak 2', and speculated V_{T2} quite matches the position of peak 3. The conductivity change of pentacene layer motives us to set up a model to detect the origins of E_1 and to investigate internal electric field distribution inside the device.

Model description

Here the model is proposed to illustrate the relationship between E_1 and V_{ex}. If there are no free carriers transporting through pentacene or P(VDF-TrFE), both two layers can be regarded as insulator. On the other hand, alteration of space charge distribution due to interfacial charge accumulation and dipole moments in ferroelectrics, influences the two layers to be insulating or not. Noteworthy that, there is actually no absolute standard to distinguish "insulating" between "conductive", it only refers to the change of conductivity due to moving carriers, rather than the perspective of semiconductor physics. For simplicity, we only consider pentacene to be insulating or conductive, and P(VDF-TrFE) to be insulating or ferroelectric.

Pentacene shows p-type semiconductor behavior with high hole conductivity: ~1 cm^2/Vs [25, 26]. LUMO level of the pentacene is quite far away from the Fermi level of Au [27], thus electron injection is unlikely and there is a substantial energy barrier for electrons [28, 29]. Therefore, if there is no charge injection from Au electrode into pentacene or no interfacial charging, pentacene shows insulating property with low electrical conductivity; otherwise, pentacene shows conductive behavior when charges (holes or electrons) are smoothly injected with high conductivity and accumulated charge at the interface.

As mentioned above, large dipole moments are perpendicular to the P(VDF-TrFE) film surface aligned to the external electric filed as a result of spin-coating method. Besides, by considering the switching speed of dipoles [30], dipole reversal smoothly happens under the current sweeping rate when electric field applied across the P(VDF-TrFE) layer reaches to coercive electric field. Therefore, P(VDF-TrFE) to be insulating or ferroelectric depends mainly on turn-over of spontaneous polarization. We manage to simplify all the conditions into four cases with Eq. [(4(a), 5(a), 5(b), 5(c)), as is concluded in Table. 1 and Fig. 3 (a).

For case I, if both pentacene layer and P(VDF-TrFE) are insulating, the potential drop across pentacene layer only originates from external voltage, $E_1 = \frac{CV}{\varepsilon_1} = E_{ex}$, as is plotted by dotted line 1 in Fig. 3 (a).

For case II, if taking into consideration of dipole polarization in P(VDF-TrFE) layer when no charge flow in the pentacene layer, polarization contributes to E_1, $E_1 = \frac{CV}{\varepsilon_1} + \frac{P}{C_1+C_2} \cdot \frac{1}{d_1}$. At position V=0, when external voltage changes into negative bias from positive bias, dipoles moments in P(VDF-TrFE) layer remain upwards, generating upwards electric field, that is, E_1 is positive and equals to E_s; on the other hand, when external voltage turns from negative to positive, E_1 is negative and also equals to E_s. Therefore, E_1 should follow two lines parallel to line 1, depicting the insulating property of pentacene and P(VDF-TrFE) layers, with two switching points connecting a loop, remarking the dipole reversal processes. At $V = V_4 = -E_c \cdot d_2 \cdot (C_1+C_2)/C_1$, dipoles switch from upwards to downwards, slowly decreasing E_1 and approaching the parallel line beneath line 1. Same thing happens at $V=V_3$, displaying a loop with symmetry, as is plotted by solid line 2 in Fig. 3 (a).

For case III, considering adequate charge injection, pentacene layer is of high conductivity, potential drop in pentacene always equals zero. That is, the interface charge Q_s contributes to E_1. $E_1 = \frac{CV}{\varepsilon_1} + \frac{Q_s}{C_1+C_2} \cdot \frac{1}{d_1}$, $Q_s = -C_2 V$, $E_1=0$, which implies that, the electric field due to the accumulated interfacial charge compensate

the external applied electric field, as is plotted by dotted line line 3 in Fig. 3 (a). This case is similar to MFM device, as pentacene is acting as a conductor, and all the external voltage is applied across P(VDF-TrFE) layer.

For case IV, it is similar to the actual case with taking into account of both P and Q_s. $E_1 = \frac{CV}{\varepsilon_1} + \frac{P}{C_1 + C_2} \cdot \frac{1}{d_1} + \frac{Q_s}{C_1 + C_2} \cdot \frac{1}{d_1}$. Here the model only depicts the ideal case with adequate interfacial charges, which are sufficient to totally compensate the electric field from other sources, keeping pentacene with high conductivity. Thus line 4 should be the same as line 3 excepts two turning points, when electric field in P(VDF-TrFE) reaches the coercive electric field for dipole switching at $V=V_1$ and $V=V_2$. In process 0 $\rightarrow V_m$, E_1 gradually increases due to the upwards E_P during dipole switching and goes back to zero as a result of E_s, which accounts for the peak. Same thing happens at $V=V_2$, as illustrated by solid line 4 in Fig. 3 (a).

The model overcomes complex assumption of capacitance variation, and basically explores the origins of the internal electric filed in the pentacene layer — external applied voltage, interfacial charging/discharging, and dipole reversal, by considering the dielectric property of the two sandwiched layers. Accordingly, this modified model paves way for analyzing detailed carrier motions. Noteworthy that, we neglected P(VDF-TrFE)/ITO interface or influence of free carriers on polarization reversal in ferroelectric film, and focused on the influence of polarization on free carriers in pentacene layer, considering the dominant contribution of polarization reversal. And we are working on improving the precision accuracy of microscopic SHG method.

EFISHG results

Fig. 3(b) demonstrates the EFISHG results for MFSM device in dark and under illumination. For in dark case, there is one peak in the positive bias and a step in the negative bias. And for under illumination case, there are two symmetric steps at both voltage regions.

In dark

The EFISHG result implies a process of modified combination of case II and case IV from the model.

For $-V_m \rightarrow 0$ process, as holes smoothly injected from Au electrode into pentacene layer, pentacene is acting as conductor, similar to line 4 pictured in the model. E_p keeps at a fixed value downwards, $\Delta E_p=0$, $\Delta E_s= -\Delta E_{ex}$, $\Delta E_1=0$, E_1 stays constant. Noteworthy that, a constant non-zero baseline of $\sqrt{I(2\omega)}$ should be subtracted (see the dotted horizontal line depicted in Fig. 3(b)). It may possibly arise from the built-in potential across the device, which is established due to the work function difference between the two electrodes or from the surface of the ITO electrode [14, 31]. Therefore, E_1 approaches zero, depending on the comparison of $E_{ex}+E_p$ and E_s, and interfacial charging process takes control.

For $0 \rightarrow V_m$ process, at first, the pentacene layer stays conductive as holes gradually expelled back to the gold electrode due to electrostatic attraction of the charge from external voltage. Also, $\Delta E_s= -\Delta E_{ex}$, and E_1 remains constant. Part of the dipoles switches from downwards to upwards at $V=V_2$, and this process is well aligned with line 4 predicted in the model. After dipole reversal, however, pentacene is becoming more insulating for: holes accumulated at the interface are accelerated to repel back to Au electrode due to the upwards E_p; On the other hand, small possibility of electron injection leads to negligible free carriers through pentacene layer. Then E_1-V_{ex} follows line 2 afterwards before approaching $V=V_3 \approx E_c \cdot d_2 \cdot (C_1+C_2)/C_1$, where the rest of the dipoles finish switching. The increasing E_1 value indicates a continuous dipole reversal process during $V=V_2$ to $V=V_3$. Different from what the model speculated, E_1 decreases after $V=V_3$, which implies a possibility of electron injection at high voltage range. The accumulated injected electrons at the interface

generate a downwards E_s, which accounts for the appearance of the peak at forward bias. Afterwards, E_1 decreases to a steady value rather than zero, indicating that as external voltage increases linearly, electron injection is smoothly injected with $\Delta E_s = -\Delta E_{ex}$. Therefore, E_1 keeps constant as a result of the balance between E_p, E_{ex} and E_s.

For $V_m \rightarrow 0$ process, the balance between E_p, E_{ex} and E_s breaks up and E_1 decreases at first. Considering the p-type semiconductor property of pentacene, electron mobility is much smaller than the hole mobility. ΔE_s fails to keep the same pace with ΔE_{ex}, and $\Delta E_s < -\Delta E_{ex}$. As a result, E_1 decreases until ΔE_{ex} and ΔE_s gradually regain a balance at a lower voltage, as electron injection may become smoothly. And this equilibrium trend continues till external voltage reaches zero.

For $0 \rightarrow -V_m$ process, as the external voltage change direction, $\Delta E_s = -\Delta E_{ex}$ and the balance remains at the begining. Noteworthy that, at some point of applied voltage, when all the electrons expelled, hole charging again takes control. At $V=V_1$, all the dipoles switch to downwards, and a step in E_1-V_{ex} characteristic shows up, which is the case similar to line 4. After the dipole reversal, $\Delta E_s = -\Delta E_{ex}$ and E_1 stays constant.

Here to mention that, despite the same balance state of E_1, the difference of the E_1 constant value at positive bias and negative bias (around +60V and -60V) is ascribed to the smooth hole injection and hindered electron injection. $|E_s|$ is smaller in the latter case, making much less contributions to compensating internal electric field distribution.

The model is instructive to clarify carrier motions by coupling with EFISHG result.

Under illumination

When exposed to white light, excitons are generated in the pentacene layer. Dissociation of holes and electrons in exciton pairs contributes to increasing the conductivity of pentacene layer. Therefore, we are expecting the E_1-V characteristics for under illumination case to be speculated in the model as line 4.

As depicted in Fig. 3(b), the EFISHG result under illumination shows a symmetric loop, which overlaps with that of in dark case for the negative bias and different from the peak in dark for positive bias. Besides the abrupt variation of E_p due to dipole reversal at $V=V_1$ and $V=V_2$, E_1 stays constant since ΔE_s always equals to $-\Delta E_{ex}$ at the entire voltage range. E_s is smaller at V= +60V than that at V= -60V under illumination, but larger than that of the in dark case. It may be inferred that interfacial charging under illumination is photogenerated carrier dominated, rather than hole/electron injection controlled. Noteworthy that, E_s at V= -60V is the same at that of in dark case, suggesting the sufficient interfacial charging regardless of the origins.

In the process of $V_m \rightarrow V_3$, the different tendency of E_1 with/without illumination further proves the ideas mentioned above. For in dark case, $\Delta E_s \neq \Delta E_{ex}$ due to the small mobility of electrons in pentacene layer, and E_1 gradually decreases; while under illumination, the space charge electric field due to the exciton pairs alignment respond much quickly to compensate E_{ex}, remaining the balance state of E_1. Noteworthy that, in the process of $V_3 \rightarrow 0$, E_1 is the exact same equilibrium value for in dark and under illumination. This also assists rationality of the balance state establishment process.

In summary, when exposed to high intensity of while illumination, pentacene layer remains to be conductive due to dissociation of holes and electrons in excitons. Both voltage ranges show identical interfacial charging process with hindered carrier injection.

***DCM* current in the low voltage region**

DCM current is quite small in the region V< -60, but not zero. Here we pay attention to this current. Fig. 2(b)

shows the result that, right after sample preparation, the first DCM test in dark for several circles, and later the second DCM test under illumination for several circles. Generally speaking, our idea suggests that this DCM current in this low voltage region includes very small leakage current and it increases under photo-illumination due to increase of photo-generated carriers. However, in our experiment, this DCM current under illumination shows no increase rather than decrease. For more detail, under the illumination, *the flowing current* at the -60V point (as marked in the Fig. 2(b)) is decreased in comparison with the *current* in dark condition. This is our finding, and further study is necessary to account for the illumination effect. Noteworthy that, results in Fig. 2(a) is conducted under repeated circles, where DCM current of in dark and under illumination are almost the same value. This maybe explained that, after repeated charging/discharging process of the device, the stability of polarization in P(VDF-TrFE), alternation of surface morphology on top Au electrode due to space charge distribution, all contribute to a final steady state of this MFSM device and small leakage current at the low voltage range.

Here we try to figure out why DCM current is even smaller under illumination compared to that in dark. The DCM current at the voltage of -60V has two origins, *conductive dc leakage current*, which is decided by the insulating performance of the devices, and *displacement current*, which is given as $I_c = C_{total}\frac{dV}{dt}$. The *conductive dc leakage current* might be insignificant due to good and photo-insensitive insulating performance of the P(VDF-TrFE) layer. Since the scanning rate of the measurement (dV/dt) is the same for two cases, the decrease of the leakage current may be attributed to the changing of the total capacitance of the device. Under illumination case, as we have discussed in the former part that excitons separation may suppress carrier injection, which leads to the decrease of the total capacitance of the device. The sharp displacement current observed in Fig. 2 also supports this assumption, since the charge storage ability is decreased under the illumination and the device is not fully discharged. This is a tentative perspective to account for the decrease of the DCM current in the low voltage region under illumination, but further studies are expected to clarify the details.

Ⅳ. CONCLUSIONS

Our researches focus on clarifying carrier behaviors in ferroelectric film inserted MFSM structures by coupling DCM and EFISHG measurement. A model was proposed to visualize and to detect the origins of the internal electric field in pentacene layer by analyzing the conductivity variation of pentacene. With high intensity illumination stimulation, dissertation of holes and electrons from excitons contributes to high conductivity of pentacene and suppressed carrier injection, which in turn affecting dipole reversal process. In addition, the same balance state of electric field in pentacene of two cases implies that despite the interfacial charging origins, space charge field distribution could not completely compensate potential drop across pentacene layer, which may also impact on leakage current through the device. More investigations on the interactive influence of photo illumination, dipole polarization and interfacial charging on adjusting internal electric filed distribution are expected, which will be helpful for further study on the application of ferroelectric films, eg, OSCs.

Acknowledgement

This research was supported by Tokyo Tech-Tsinghua University Joint Graduate Program. In addition, Daikin Kogyo Co., Ltd. was highly appreciated for supplying P(VDF-TrFE) copolymers.

Reference

[1] K. Henkel, I. Lazareva, D. Mandal, I. Paloumpa, K. Müller, Y. Koval, P. Müller, D. Schmeißer, J. Vac. Sci. Technol. B. 27 (2009) 504
[2] J. C. Lee, N. G. Subramaniam, J. W. Lee, T. W. Kang, Appl. Phys. Lett. 90 (2007) 262909
[3] X. Chen, M. Iwamoto, Z. Shi, L. Zhang, Z. L. Wang, Adv. Funct. Mater. 25 (2015) 739
[4] Y. Yuan, T. J. Reece, P. Sharma, S. Poddar, S Ducharme, A. Gruverman, Y. Yang, J. Huang, Nature Mater. 10 (2011) 296
[5] K. S. Nalwa, J. A. Carr, R. C. Mahadevapuram, H. K. Kodali, S. Bose, Y. Chen, J. W. Petrich, B. Ganapathysubramanian, S. Chaudhary, Energy Environ. Sci. 5 (2012) 7042
[6] T. Yamada, T. Kitayama, J. Appl. Phys. 52 (1981) 6859
[7] T. Furukawa, M. Date, G. E. Johnson, J. Appl. Phys. 54 (1983) 1540
[8] K. Kimura, H. Ohigashi, Appl. Phys. Lett. 43 (1983) 834
[9] J. F. Legrand, Ferroelectrics, 91 (1989) 303
[10] M. Iwamoto, T. Manaka, D. Taguchi, J. Phys. D: Appl. Phys. 48 (2015) 373001
[11] T. Manaka, E. Lim, R. Tamura, D. Yamada, M. Iwamoto, Appl. Phys. Lett. 89 (2006) 072113
[12] D. Taguchi, T. Shino, X. Chen, L. Zhang, J. Li, M. Weis, T. Manaka, M. Iwamoto, J. Appl. Phys. 110 (2011) 103717
[13] J. Li, L. Zhang, W. Ou-Yang, D. Taguchi, T. Manaka, M. Iwamoto, Jpn. J. Appl. Phys. 49 (2010) 121601
[14] J. Li, W. Ou-Yang, T. Manaka, M. Iwamoto, Appl. Phys. Lett. 99 (2011) 063302
[15] J. Li, M. Weis, D. Taguchi, T. Manaka, M. Iwamoto, J. Appl. Phys. 111 (2012) 023706
[16] M. Weis, J. Li, D. Taguchi, T. Manaka, M. Iwamoto, Appl. Phys. Express. 4 (2011) 121601
[17] K. Koga, N. Nakano, T. Hattori, H. Ohigashi, J. Appl. Phys. 67 (1990) 965
[18] H. Ohigashi, K. Koga, Jpn. J. Appl. Phys. 21 (1982) 455
[19] J. Gao, F. A. Hegmann, Appl. Phys. Lett. 93 (2008) 223306
[20] J. F. Legrand, Ferroelectrics 91 (1989) 303
[21] Y. R. Shen, The Principles of Nonlinear Optics (Wiley, New York, 1984)
[22] F. Michelotti, L. Dominici, A. Belardini, AIP Conf. Proc. 709 (2004) 233
[23] W. Li, Y. Zhu, D. Hua, P. Wang, X. Chen, J. Shen, Appl. Surf. Sci. 254 (2008) 7321
[24] D. Mao, M. A. Quevedo-Lopez, H. Stiegler, B. E. Gnade, H. N. Alshareef, Org. Electron. 11 (2010) 925
[25] H. -S. Seo, Y. -S. Jang, Y. Zhang, P. S. Abthagir, J. –H. Choi, Org. Electron. 9 (2008) 432
[26] Y. -J. Lin, H. -Y. Tsao, D. -S. Liu, Appl. Phys. Lett, 101 (2012) 013302
[27] A. Kahn, N. Koch, W. Gao, J. Polym. Sci. B. Polym. Phys. 41 (2003) 2529
[28] T. Manaka, F. Liu, M. Weis, M. Iwamoto, J. Phys. Chem. C. 113 (2009) 10279
[29] X. Chen, D. Taguchi, T. Manaka, M. Iwamoto, Appl. Phys. Lett. 104 (2014) 013306
[30] T. Furukawa, H. Matsuzaki, M. Shiina, Y. Tajitsu, Jpn. J. Appl. Phys. 24 (1985) L661
[31] F. Ghebremichael, C. Poga, M. G. Kuzyk, Appl. Phys. Lett. 66 (1995) 139

Table and Figure captions

Table 1 Model description based on dielectric physics.

Figure 1 Sample structure of Pentacene/P(VDF-TrFE) MFMS device for experimental arrangement; the inset shows the manner of applied ramp voltage in DCM and EFISHG measurement. Note that V is defined as positive as illustrated, P and E is set positive as upwards, Qs is positive when holes accumulated at the interface.

Figure 2 DCM results at the frequency of 10 mHz for (a) MFM device and MFSM device in dark and under illumination after repeated measuring circles; (b) MFSM device with in dark for the first several testing circles and under illumination for the second several circles.

Figure 3 (a) Model for for E1-V characteristics. Line1~4 depicts cases Ⅰ～Ⅳ, respectively. The dashed four lines, V=Vn(n=1~4), represent the turn-over voltage for dipole reversal, with $V1 \approx -V2=VT1= Ec \cdot d2$, $V3 \approx -V4=VT2= Ec \cdot d2 \cdot (C1+C2)/C1$. Line 3 overlapped with part of line 4. (b) EFISHG results for MFSM device in dark and under illumination. The dashed horizontal line depicts the square-root SH level of background noise.

Table.1 Model description based on dielectric physics.

Case	Pentacene	P(VDF-TrFE)	Q_s	P	E_1	Depiction
Ⅰ	insulating	insulating	$Q_s=0$	P=0	$E_1=\frac{CV}{\varepsilon_1}=E_{ex}$	Line 1
Ⅱ	insulating	ferroelectric	$Q_s=0$	P≠0	$E_1=\frac{CV}{\varepsilon_1}+\frac{P}{C_1+C_2}\cdot\frac{1}{d_1}$	Line 2
Ⅲ	conductive	insulating	$Q_s\neq0$	P=0	$E_1=\frac{CV}{\varepsilon_1}+\frac{Q_s}{C_1+C_2}\cdot\frac{1}{d_1}$	Line 3
Ⅳ	conductive	ferroelectric	$Q_s\neq0$	P≠0	$E_1=\frac{CV}{\varepsilon_1}+\frac{P}{C_1+C_2}\cdot\frac{1}{d_1}+\frac{Q_s}{C_1+C_2}\cdot\frac{1}{d_1}$	Line 4

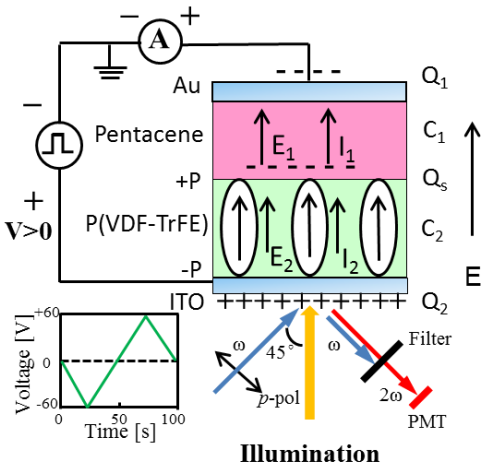

Fig.1 Sample structure of Pentacene/P(VDF-TrFE) MFMS device for experimental arrangement; the inset shows the manner of applied ramp voltage in DCM and EFISHG measurement. Note that V is defined as positive as illustrated, P and E is set positive as upwards, Qs is positive when holes accumulated at the interface.

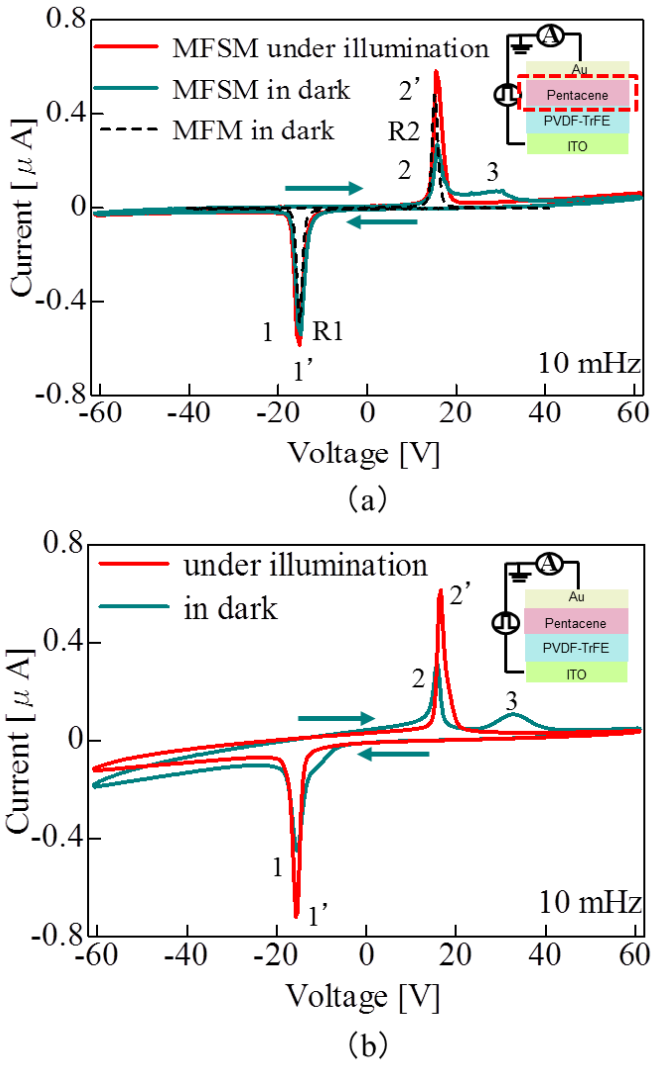

Fig.2 DCM results at the frequency of 10 mHz for (a) MFM device and MFSM device in dark and under illumination after repeated measuring circles; (b) MFSM device with in dark for the first several testing circles and under illumination for the second several testing circles.

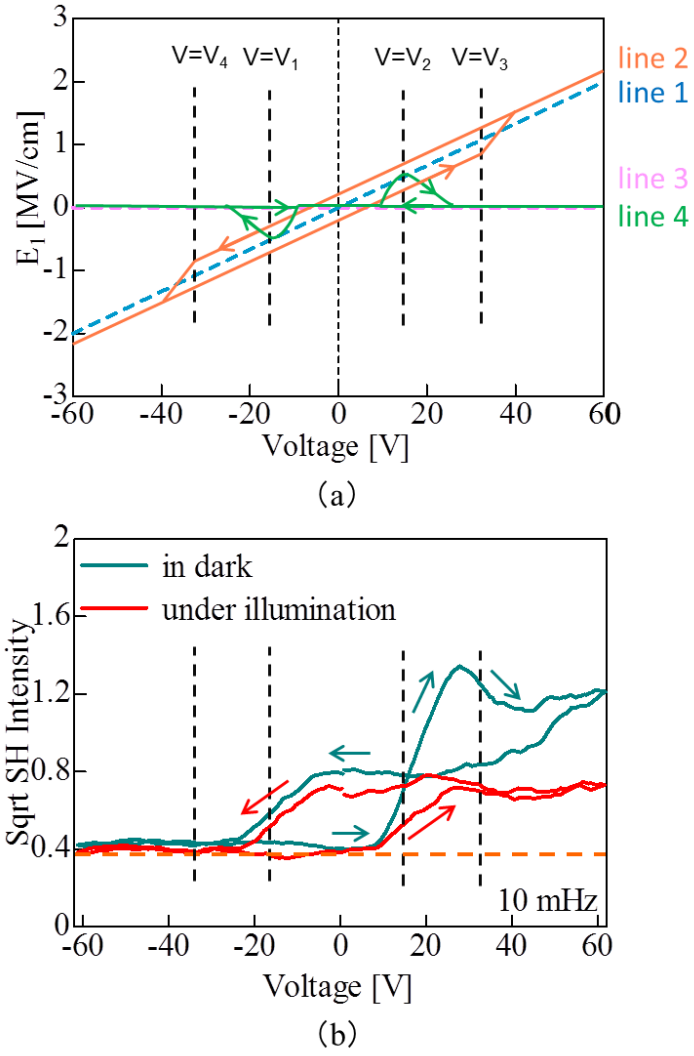

Fig.3. (a) Model for for E_1-V characteristics. Line1~4 depicts cases Ⅰ～Ⅳ, respectively. The dashed four lines, $V=V_n(n=1\sim4)$, represent the turn-over voltage for dipole reversal, with $V_1\approx-V_2=V_{T1}= E_c\cdot d_2$, $V_3\approx-V_4=V_{T2}= E_c\cdot d_2\cdot(C_1+C_2)/C_1$. Line 3 overlapped with part of line 4. (b) EFISHG results for MFSM device in dark and under illumination. The dashed horizontal line depicts the square-root SH level of background noise.